Paper pa03-049
Submitted to the 28th International Conference on High Energy Physics
ICHEP'96, Warsaw, Poland, July 1996

Forward Jet Production at HERA

H1 Collaboration

Abstract

One of the advocated footprints of BFKL dynamics in deep inelastic electron proton collisions is the measurement of forward jet cross sections and characteristics. Forward jets are jets which are produced with a small angle with respect to the incident proton direction. Forward jet cross sections, measured with the H1 detector are presented as function of Bjorken-x, for jets produced with an angle to the proton direction, Θ_{jet}, in the range $7 < \Theta_{\mathrm{jet}} < 20$ degrees. The cross sections are determined for various values of the minimum jet transverse energy. The results are compared with predictions of analytical BFKL calculations and QCD based Monte Carlo calculations.

1 Introduction

The electron-proton collider HERA has opened new kinematical regions to study Deep Inelastic Scattering (DIS): the regions of large four-momentum transfer Q^2 (up to $Q^2 \approx 10^4$ GeV^2) and small Bjorken-x ($x \approx 10^{-4}$). The region of small x has been suggested to be sensitive to new dynamic features of QCD [1]. The ZEUS and H1 collaborations have observed [2, 3] that the proton structure function F_2 exhibits a strong rise towards small Bjorken-x. This rise has caused much debate on whether the HERA data are still in a regime where the QCD evolution of the parton densities can be described by the DGLAP (Dokshitzer-Gribov-Lipatov-Altarelli-Parisi) [4] evolution equations, or whether they extend into a new regime where the QCD dynamics is described by the BFKL (Balitsky-Fadin-Kuraev-Lipatov) [5] evolution equation. The BFKL evolution equation is expected to become applicable in the region at small x, since it resums all $\ln 1/x$ terms in the perturbative expansion, contrary to the DGLAP equation. It has turned out however that present F_2 measurements do not yet allow to discriminator between BFKL and conventional DGLAP dynamics [6], and are perhaps a too inclusive measurement to be a sensitive discriminator. Hadronic final states have been suggested to give additional information and be more sensitive to the parton evolution [7, 8]. In this paper we use the H1 detector to study the production of forward jets.

For events at low x, hadron production in the region between the current jet and the proton remnant is expected to be sensitive to effects of the BFKL or DGLAP dynamics. At lowest order the BFKL and DGLAP evolution equations effectively resum the leading logarithms $\alpha_s \ln 1/x$ or $\alpha_s \ln Q^2$ contributions respectively which, in an axial gauge, amounts to a resummation of ladder diagrams of the type shown in Fig. 1. It shows that before a quark is struck by the virtual photon, a cascade of partons may be emitted. The proton momentum fractions x_i and transverse momenta k_{Ti} of the emitted partons are indicated in the figure. In the leading log DGLAP scheme this parton cascade follows a strong ordering in transverse momentum $k_{Tn}^2 \gg k_{Tn-1}^2 \gg ... \gg k_{T1}^2$, while there is only a soft (kinematical) ordering for the fractional momentum $x_n < x_{n-1} < ... < x_1$. For the BFKL scheme the cascade follows a strong ordering in fractional momentum $x_n \ll x_{n-1} \ll ... \ll x_1$, while there is no ordering in transverse momentum [9]. The transverse momentum follows a kind of random walk in k_T space: the k_{Ti} value is close to the k_{Ti-1} value, but it can be both larger or smaller [10].

A possible footprint of the BFKL dynamics is the rate of jets produced in DIS, with the following characteristics [7, 8, 11], designed to suppress the phase space for jet production resulting from the DGLAP evolution compared to the one in case of BFKL evolution. Due to the strong ordering, the condition $k_{T\mathrm{jet}}^2 \approx Q^2$ leaves little room for DGLAP evolution. The momentum fraction of the jet, $x_{\mathrm{jet}} = E_{\mathrm{jet}}/E_p$, should be as large as possible, whereas the momentum fraction x of the quark struck by the virtual photon should be small, in order to maximize the phase space for jet production from BFKL evolution which is governed by the ratio x_{jet}/x. Here E_{jet} and E_p are the energies of the jet and the incoming proton respectively. Hence the rate of events at small x with a jet at high x_{jet} is expected to be higher for the BFKL than for the DGLAP scenario.

The data can be compared with analytical calculations [12] at the parton level. Predictions for final state observables are also available as Monte Carlo models, based upon QCD phenomenology. In this report we will refer to three of the currently available Monte

Carlo programs: the MEPS (Matrix Elements plus Parton Showers), the CDM (Colour Dipole Model) and HERWIG models. The CDM model [13] provides an implementation of the colour dipole model of a chain of independently radiating dipoles formed by emitted gluons [14]. Since all radiation is assumed to come from the dipole formed by the struck quark and the remnant, photon-gluon fusion events have to be added and are taken from the QCD matrix elements [15]. It has been suggested that CDM approaches more the BFKL type of evolution, because the gluons emitted by the dipole radiation do not obey strong ordering in k_T [16], although it does not explicitly make use of the BFKL evolution equation. The MEPS model is an option of the LEPTO generator [15] based on DGLAP dynamics. It has to be pointed out that the DGLAP formalism is derived for the totally inclusive structure function evolution, and it can be questioned whether it is fully applicable for exclusive final states [17]. MEPS incorporates the QCD matrix elements up to first order, with additional soft emissions generated by adding leading log parton showers. The emitted partons are strongly ordered in k_T. Both the MEPS and CDM models use the Lund string model [18] for hadronizing the partonic final state. The HERWIG model [19] is also based upon leading log parton showers, with additional matrix element corrections. This model implements an alternative (cluster) fragmentation scheme. The models are used in their latest versions (LEPTO6.4 for MEPS, and HERWIG 5.8d). The CDM model is used via the generator DJANGO6 [20], and noted as DJ6-CDM in the figures. As input for the generators the parton density parametrization GRV [21] is used, which results in a good description of the HERA F_2 measurements[2, 3].

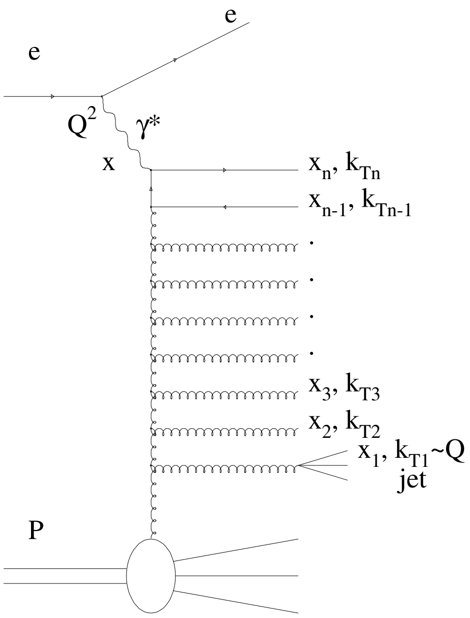

Figure 1: Parton evolution in the ladder approximation. The selection of forward jets in DIS events is illustrated.

Experimental data for this analysis were collected by H1 during the 1994 running period, in which HERA collided 27.5 GeV positrons on 820 GeV protons, thus producing e^+p interactions at $\sqrt{s} = 300$ GeV. The data sample used corresponds to an integrated luminosity of 2.8 pb^{-1}.

2 The H1 Detector

A detailed description of the H1 apparatus can be found elsewhere [22]. The following briefly describes the components of the detector relevant to this analysis.

The hadronic energy flow and the scattered electrons are measured with a liquid argon (LAr) calorimeter and a backward electromagnetic lead-scintillator calorimeter (BEMC). The LAr calorimeter [23] extends over the polar angular range $4^\circ < \theta < 153^\circ$ with full azimuthal coverage, where θ is defined with respect to the proton beam direction ($+z$ axis). It consists of an electromagnetic section with lead absorbers and a hadronic section with steel absorbers. Both sections are highly segmented in the transverse and the longitudinal direction with about 44000 cells in total. The total depth of both calorimeters varies between 4.5 and 8 interaction lengths. Test beam measurements of the LAr calorimeter modules show an energy resolution of $\sigma_E/E \approx 0.50/\sqrt{E\text{ [GeV]}} \oplus 0.02$ for charged pions [22, 23, 24]. The hadronic energy measurement is performed by applying a weighting technique in order to account for the non-compensating nature of the calorimeter. The absolute scale of the hadronic energy is presently known to 5%, as determined from studies of the transverse momentum (p_T) balance in DIS events. This was verified by comparing the energy deposition of isolated charged tracks with their momenta measured in the central drift chamber.

The BEMC (depth of 22 radiation lengths or 1 interaction length) covers the backward region of the detector, $151^\circ < \theta < 177^\circ$. A major task of the BEMC is to trigger and to measure scattered electrons in DIS processes with Q^2 values ranging from 5 to 100 GeV^2. The BEMC energy scale for electrons is known to an accuracy of 1%. Its resolution is given by $\sigma_E/E = 0.10/\sqrt{E\text{ [GeV]}} \oplus 0.42/E\text{[GeV]} \oplus 0.03$ [25].

The calorimeters are surrounded by a superconducting solenoid providing a uniform magnetic field of 1.15 T parallel to the beam axis in the tracking region. Charged particle tracks are measured in a central drift chamber and the forward tracking system, covering the polar angular range $7^\circ < \theta < 165^\circ$. A backward proportional chamber (BPC), in front of the BEMC with an angular acceptance of $155.5^\circ < \theta < 174.5^\circ$ serves to identify electrons and to precisely measure their direction. Using information from the BPC, the BEMC and the reconstructed event vertex the polar angle of the scattered electron is known to about 1 mrad.

The luminosity is measured with the reaction $ep \to ep\gamma$ with two TlCl/TlBr crystal calorimeters, installed in the HERA tunnel. The electron tagger is located at $z = -33$ m and the photon tagger at $z = -103$ m from the interaction point in the direction of outgoing positron beam.

3 Results and Discussion

Forward jets have been studied in a sample of DIS events with a scattered electron satisfying $E_e > 11$ GeV, $160^0 < \theta_e < 173^0$ and kinematics in the region $y > 0.1$ and $0.0005 < x < 0.0035$. The cut on the inelasticity variable y ensures that for non-radiative events the current quark jet is more central and well separated from the forward jet. A cone algorithm is used to find jets in the H1 calorimeter, requiring an E_T larger than

3.5 GeV in a cone of radius $R = \sqrt{\Delta\eta^2 + \Delta\phi^2} = 1.0$ in the space of pseudo-rapidity η and azimuthal angle ϕ in the HERA frame of reference. We have measured the cross section for events which have a "forward" jet defined by $x_{\rm jet} = E_{\rm jet}/E_p > 0.035$, $0.5 < p_{T\rm jet}^2/Q^2 < 2$, $7^0 < \Theta_{\rm jet} < 20^0$ and $p_{T\rm jet} > 3.5, 5$ and 6 GeV, where $p_{T\rm jet}$ is the transverse momentum of the jet, assumed to be equal to E_T, and E_p is the incident proton energy. The data are corrected for detector effects using events generated with the CDM model for which the detector response was fully simulated.

The transverse energy flow around the forward jet axis, averaged over all selected events, is shown versus η and φ in Fig. 2, for different values of $p_{T\rm jet}$. Distinct jet profiles are observed, which are well described by the Monte Carlo model.

The preliminary data for $p_{T\rm jet} = 3.5$ GeV are shown as function of Bjorken-x in Fig. 3. The data points are the cross section as measured in the given x bin for the kinematic cuts and jet cuts defined above (and in the figure insert). The full errors are the quadratic sum of the statistical (inner error bars) and systematical errors. Systematic studies include the lepton and hadron energy scale and angles and different models to correct for detector effects. The systematic error is dominated by the 5% uncertainty for the hadronic energy scale. The data clearly rise with decreasing x. Backgrounds from photoproduction and radiative events (for which the current jet gets boosted into the forward region) have been studied with Monte Carlo and with. A fraction of those events can be tagged using the detectors of the luminosity system: for radiative events with a with a photon emitted collinear with the incident electron, the photon can be detected with the photon tagger; for photoproduction events the electron which is scattered under a small angle can be detected in the electron tagger. Using data samples with tagged events allows to control the Monte Carlo based estimates of the background. The background is found to be less than (3%) and subtracted from the data presented in Fig. 3.

The data are compared with Monte Carlo models and with recent analytical BFKL-calculations [12]. The data rise faster with decreasing x than HERWIG and LEPTO, two models which are based on LO-DGLAP dynamics. CDM is slightly below the data but follows the rise towards low-x. Unlike LO-DGLAP based models, this model does not include a p_T ordered cascade, and is expected to be close to the BFKL prediction. The analytical calculation is based on asymptotic expressions derived from the BFKL equation which resums the leading logarithms. For the calculation labelled "Born" no gluon was allowed to be emitted in the ladder, and corresponds to the quark box diagram seen by the photon, and one single gluon at the low end of the diagram (see ref. [12]). These calculations are at the parton level. The Born calculation clearly has a less steep slope while the BFKL calculation is more in accord with the data. However, to draw a conclusion from these data the BFKL results would need to be known at the hadron level, e.g. by using a Monte Carlo program. This is as yet not available.

In Figs. 4 and 5 preliminary forward jet cross sections are shown for different $p_{T\rm jet}$ cuts and compared with Monte Carlo models and analytical calculations. The statistics allows to present only 2 bins for the highest $p_{T\rm jet}$ cut. Therefore to ease the comparison the data are shown in two bins for all $p_{T\rm jet}$ cut values. It is clearly seen that the slope becomes smaller as $p_{T\rm jet}$ increases. Both the models and the analytical calculations follow this trend. The data are above the models for all $p_{T\rm jet}$ values.

4 Summary

A new preliminary measurement of forward jet rates as function of x has been presented, for different $p_{T\mathrm{jet}}$ cuts. The data are compared with Monte Carlo models and analytical calculations. The DGLAP based models differ in shape compared to data, while the CDM model is closer to the data. Analytical calculations at the parton level show a similar rise with decreasing x as the data. A BFKL based Monte Carlo is needed to make a direct comparisons.

References

[1] J. Bartels and J. Feltesse, Proceedings of the Workshop *Physics at HERA*, ed. W. Buchmüller and G. Ingelman, Hamburg (1992) 133;
E.M. Levin, Proc. QCD – 20 Years Later, eds. P.M. Zerwas and H.A. Kastrup, Aachen (1992), vol. 1, p. 310.

[2] H1 Collab., S. Aid et al., Nucl. Phys. B470 (1996) 3.

[3] ZEUS Collab., M. Derrick et al., DESY preprint 96-76

[4] Yu. L. Dokshitzer, Sov. Phys. JETP 46 (1977) 641;
V.N. Gribov and L.N. Lipatov, Sov. J. Nucl. Phys. 15 (1972) 438 and 675;
G. Altarelli and G. Parisi, Nucl. Phys. 126 (1977) 297.

[5] E.A. Kuraev, L.N. Lipatov and V.S. Fadin, Sov. Phys. JETP 45 (1972) 199;
Y.Y. Balitsky and L.N. Lipatov, Sov. J. Nucl. Phys. 28 (1978) 282.

[6] A.J. Askew, J. Kwieciński, A.D. Martin, P.J. Sutton, Phys. Lett. B325 (1994) 212

[7] A.H. Mueller, Nucl. Phys. B (Proc. Suppl.) 18C (1990) 125; J. Phys. G17 (1991) 1443.

[8] J. Kwieciński, A.D. Martin, P.J. Sutton, Phys. Rev. D46 (1992) 921.

[9] A.H. Mueller, Columbia preprint CU-TP-658 (1994).

[10] J. Bartels, H. Lotter, Phys. Lett. B309 (1993) 400.

[11] J. Bartels, A. De Roeck, M. Loewe, Z. Phys. **C54** (1992) 635;
W.K. Tang, Phys. Lett. B278 (1992) 363.

[12] J. Bartels et al., DESY preprint DESY096-036 (1996).

[13] L. Lönnblad, Computer Phys. Comm. 71 (1992) 15.

[14] G. Gustafson, Phys. Lett. B175 (1986) 453;
B. Andersson, G. Gustafson, L. Lönnblad and Ulf Petterson, Z. Phys. C43 (1989) 625.

[15] G. Ingelman, Proc. of the HERA workshop, eds. W. Buchmüller and G. Ingelman, Hamburg (1991) vol. 3, p. 1366.

[16] L. Lönnblad, Z. Phys. C65 (1995) 285;
A. H. Mueller, Nucl. Phys. B415 (1994) 373;
L. Lönnblad, CERN preprint CERN-TH/95-95.

[17] A. Edin, G. Ingelman and J. Rathsman, Phys. Lett. B336 (1996) 371;
A. Edin, G. Ingelman and J. Rathsman, DESY 96-060.

[18] T. Sjöstrand, Comp. Phys. Comm. 39 (1986) 347;
T. Sjöstrand and M. Bengtsson, Comp. Phys. Comm. 43 (1987) 367;
T. Sjöstrand, CERN-TH-6488-92 (1992).

[19] M. Seymour, Lund preprint LU-TP-94-12 (1994);
M. Seymour, Nucl. Phys. B436 (1995) 443.

[20] G.A. Schuler and H. Spiesberger, Proc. of the HERA Workshop, Vol 3. , Eds. W. Buchm"uller and G. Ingelman, DESY 1992, 1419

[21] M. Glück, E. Reya and A. Vogt, Z. Phys **C67** (1995) 433;

[22] H1 Collab., I. Abt et al., DESY 93-103 (1993).

[23] H1 Calorimeter Group, B. Andrieu et al., Nucl. Instr. and Meth. A336 (1993) 460.

[24] H1 Calorimeter Group, B. Andrieu et al., Nucl. Instr. and Meth. A336 (1993) 499.

[25] H1 Collab., I. Abt et al., Nucl. Phys. B407 (1993) 515.

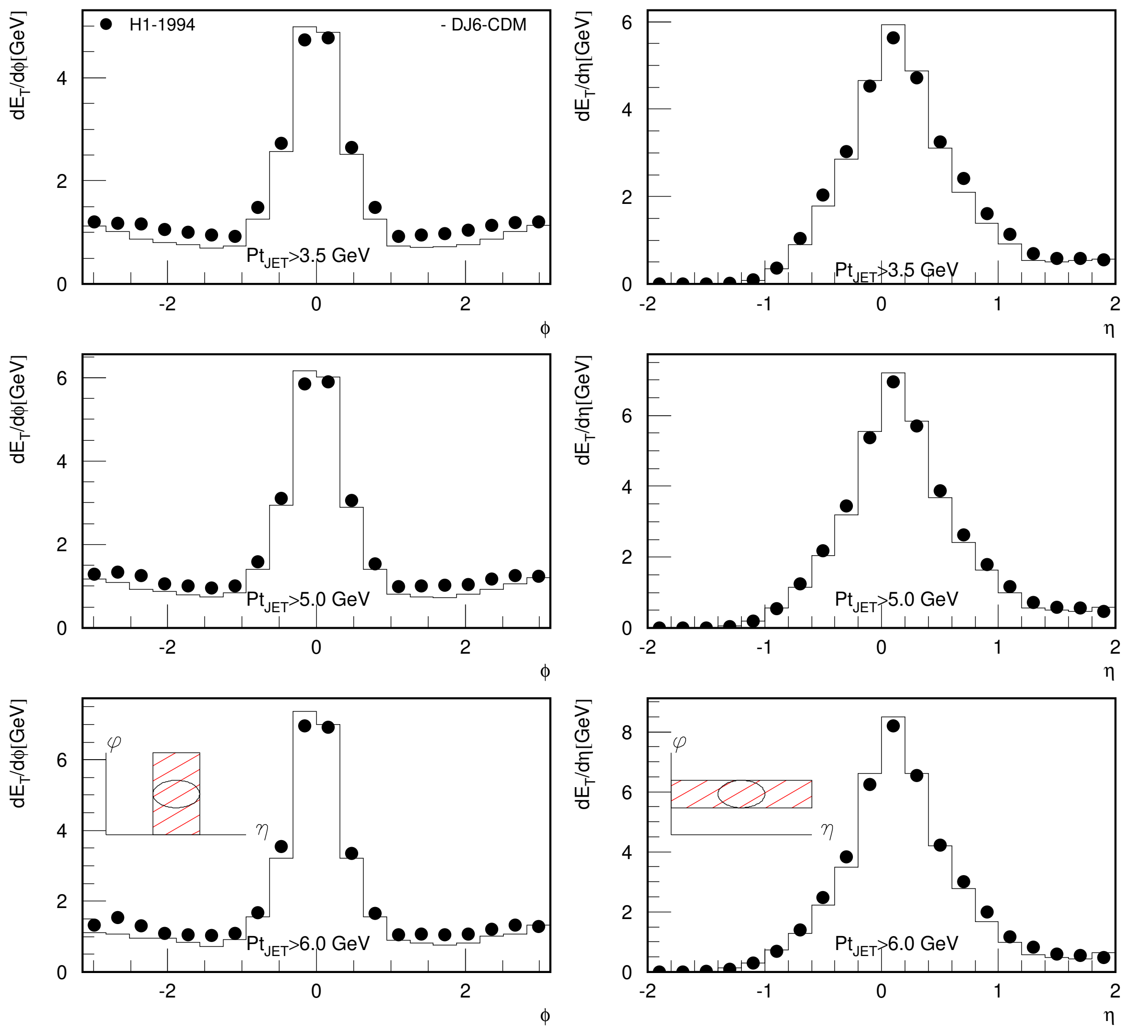

Figure 2: The average energy flow (preliminary) around the the forward jet axis over all events is shown for three different $p_{T\mathrm{jet}}$ values (right) as a function of Δeta , integrated over $|\varphi| < 1$ and (left) as a function of $\Delta\varphi$, integrated over $|\eta| < 1$. Here $\Delta\eta$ and $\Delta\varphi$ are measured with respect to the reconstructed jet axis. Also shown as the histogram is the simulation of the data in the H1 detector using the colour dipople model (DJ6-CDM).

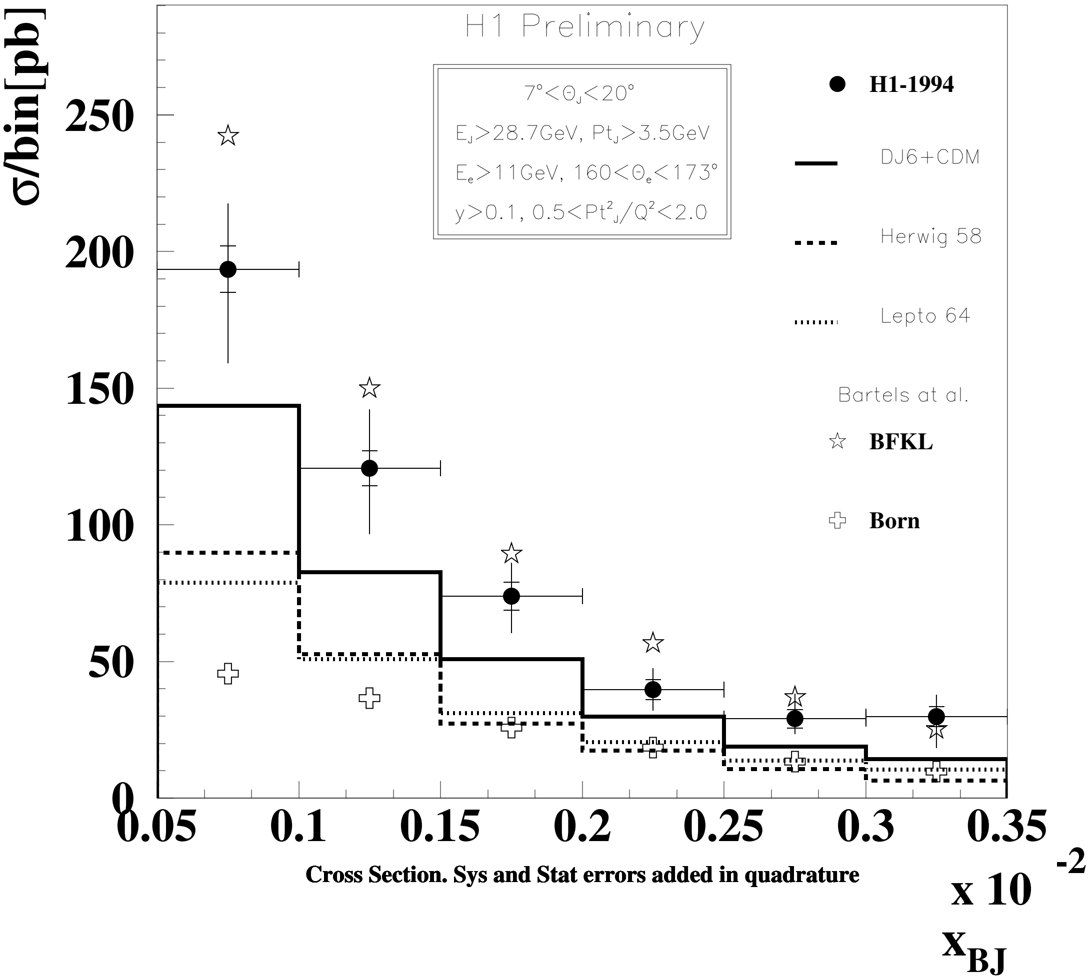

Figure 3: The preliminary forward jet cross section per bin as function of Bjorken-x; the errors of the data shown are the statistical and systematic errors added in quadrature. The curves are model calculations (full line CDM, dashed line HERWIG and dotted line LEPTO) and stars and crosses are analytical calculations, described in the text.

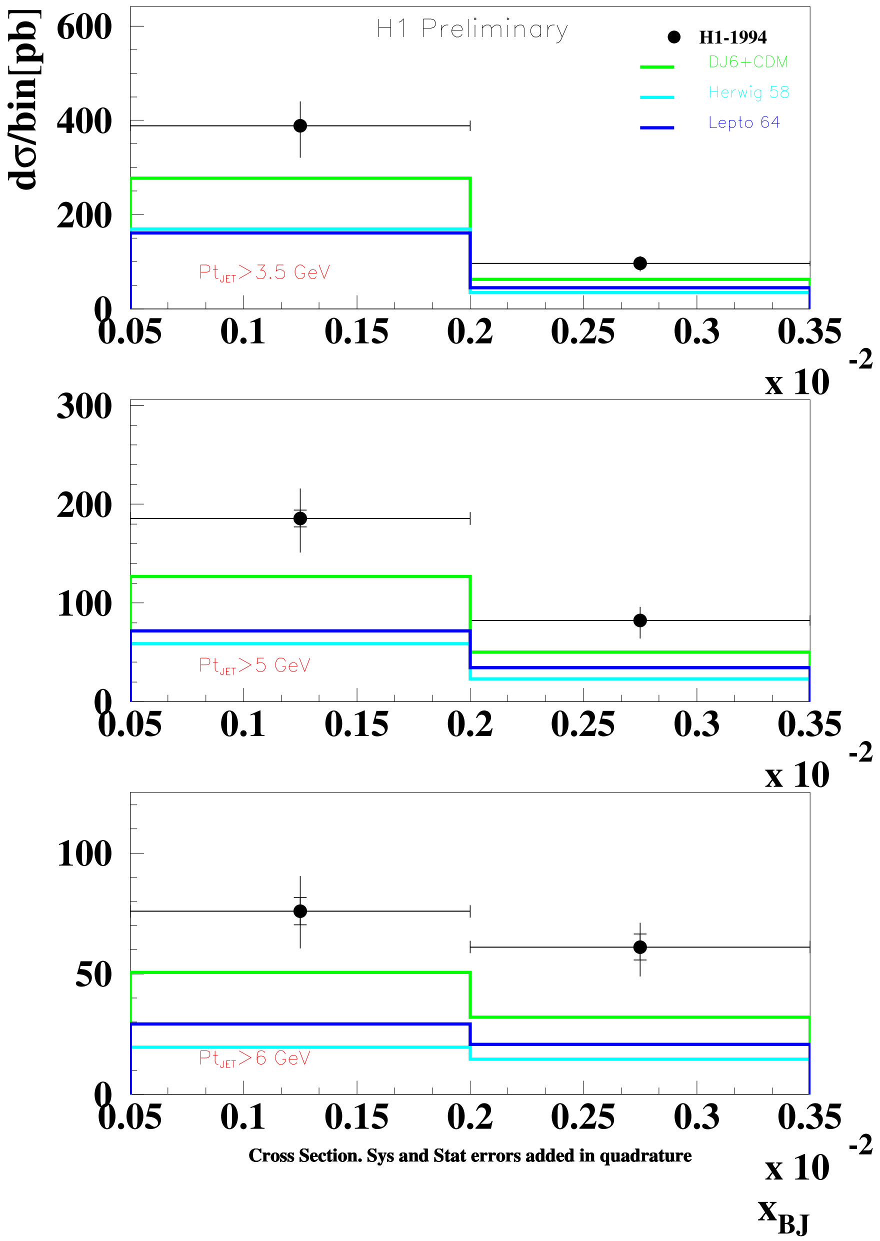

Figure 4: The preliminary forward jet cross section per bin as function of Bjorken-x for different values of $p_{T\mathrm{jet}}$; the errors shown are the statistical and systematic errors added in quadrature. The curves are model calculations (full line LEPTO, top line CDM, bottom line HERWIG), described in the text.

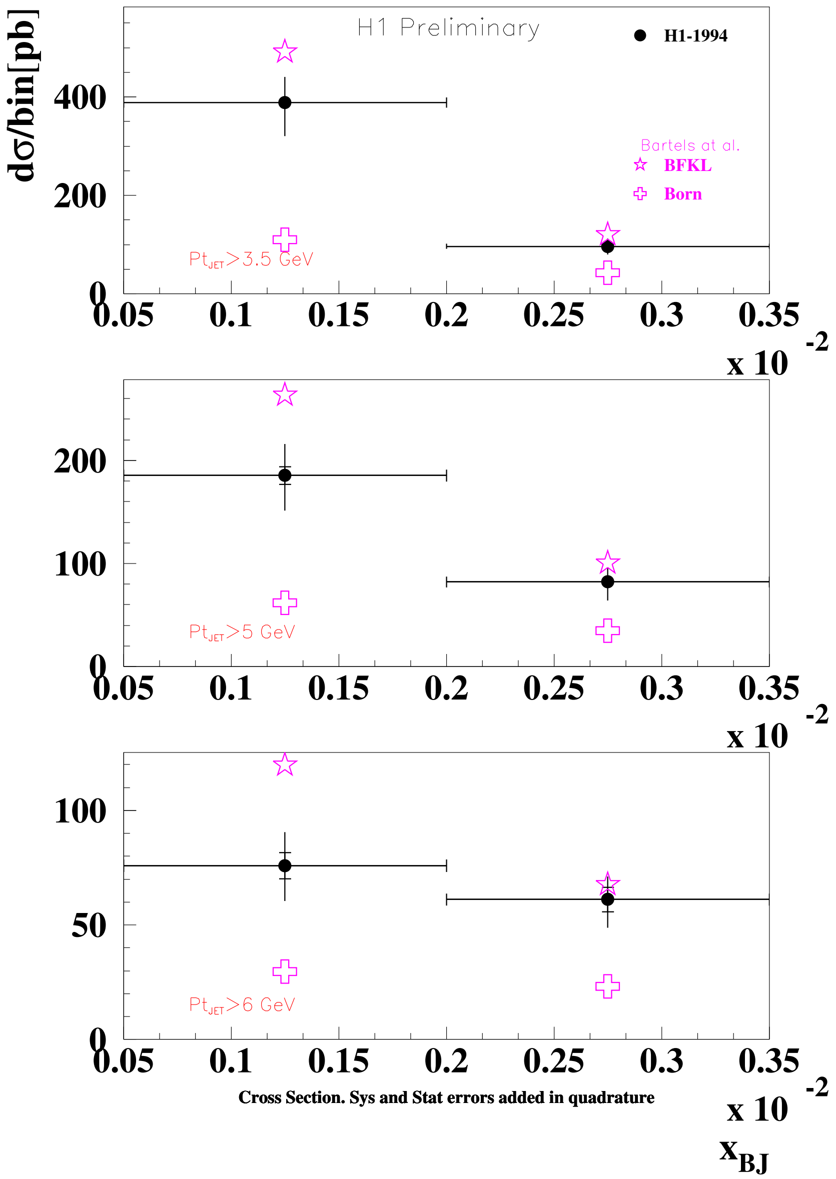

Figure 5: The preliminary forward jet cross section per bin as function of Bjorken-x for different values of $p_{T\mathrm{jet}}$; the errors shown are the statistical and systematic errors added in quadrature. The stars and crosses are analytical BFKL and "Born" calculations respectively, described in the text.